Improved conditionally replicative adenovirus delivery system against hepatocellular carcinoma by armed with bispecific T-cell engager

Xiangfei Yuan (yuanxiangfei100@163.com)
Tianjin Medical University NanKai Hospital
Yang Lu
Chinese Academy of Medical Sciences & Peking Union Medical College
Yuanyuan Yang
Tianjin Medical University General Hospital
Wencong Tian
Nankai University
Dongmei Fan
Chinese Academy of Medical Sciences & Peking Union Medical College
Ruoqi Liu
Chinese Academy of Medical Sciences & Peking Union Medical College
Xiaomin Lei
Chinese Academy of Medical Sciences & Peking Union Medical College
Yafei Xia
Integrated Chinese and Western Medicine Hospital, Tianjin University
Lei Yang
Tianjin Medical University NanKai Hospital
Shu Yan
Integrated Chinese and Western Medicine Hospital, Tianjin University
Dongsheng Xiong
Chinese Academy of Medical Sciences & Peking Union Medical College

Research Article

Keywords:

Posted Date: June 2nd, 2022

DOI: https://doi.org/10.21203/rs.3.rs-1702175/v1

Abstract

Background

Recently, many strategies have emerged to develop the conventional treatment of hepatocellular carcinoma (HCC). Previously, we have established an HCC targeting system of conditionally replicative adenovirus (CRAd) delivered by human umbilical cord-derived mesenchymal stem cells (HUMSCs). At present, the system needs to be developed for enhancing anti-tumor effect and overcoming limitation caused by alpha-fetoprotein (AFP) heterogeneity of HCC.

Methods

A bispecific T cell engager (BiTE) targeting programmed death ligand 1 (PD-L1) controlled by human telomerase reverse transcriptase (hTERT) promoter was armed on the CRAd of old system. A series of experiments *in vitro* such as ELISA, flow cytometry, electron microscope and so on were performed for identification of the novel system. Then the anti-tumor effect was explored on orthotopic transplantation model mice and AFP heterogeneous model mice by bioluminescent imaging and the side effects were assessed by levels of serum AST and ALT and HE staining for extrahepatic organs. The distributions of CRAd and BiTE in tumor tissue were detected using confocal microscope and the intratumoral T cell was analyzed by flow cytometry.

Results

Firstly, the characters of the new system including the selective killing activity of CRAd, the release of BiTE and the CRAd package and delivery by HUMSC were identified. And then the result on orthotopic transplantation model mice showed that the new system had better anti-tumor activity and less hepatotoxicity than the old. In the tumor tissue of model mice treated by the new system, the infiltration and activation of T cells were significantly enhanced. Lastly, the new system could eliminate the AFP negative cells in AFP heterogeneous tumor efficiently.

Conclusions

Comparing the old system, the new provides a more effective and safer strategy against HCC.

Background

Hepatocellular carcinoma (HCC) is a leading cause of cancer-related death in many parts of the world [1]. Due to the high rate of recurrence and metastasis of HCC and resistance to antitumor drugs, the 5-years survival rate of HCC patients is low [2]. Recently, many novel strategies have emerged to develop the

treatment of HCC [3–5]. In our previous studies, an HCC targeting system of conditionally replicative adenovirus (CRAd) delivered by human umbilical cord-derived mesenchymal stem cells (HUMSCs) has been established, which depends on the homing and hepatic differentiation of HUMSCs at tumor site and the specific transcriptional activity of alpha-fetoprotein (AFP) promoter in differentiated HUMSCs and hepatoma cells [6]. However, it is thought that the anti-tumor effect of this system should be further strengthened. Additionally, the AFP heterogeneity in hepatoma tissue will be a challenge to the clinic application of this targeting system, because the CRAds selectively clear the AFP positive tumor cells but not the negative ones. Therefore, the targeting system needs to be developed by arming with additional anti-tumor element.

In recent years, oncolytic adenovirus armed with bispecific T cell engager (BiTE) has been investigated for treatment to many solid tumors [7–9]. BiTE is a chimeric protein composed of two single-chain variable fragments (scFvs) connected with a flexible peptide linker, one of which is specific for tumor-associated antigen and the other for CD3 [10]. As well known, oncolytic virotherapy is able to evoke anti-tumor immune responses and increase the intratumoral infiltration of T lymphocytes [11–13]. When BiTE is armed on, the intratumoral T cells can be activated and selectively eliminate the tumor cells. Consequently, these properties of oncolytic adenovirus and BiTE are ideal for combinatorial approaches.

We have reported that αCD3HAC, a BiTE specific for programmed death ligand 1 (PD-L1) and CD3, was applicated in treatment against triple-negative breast cancer (TNBC) by blocking PD-L1 and activating T cells [14]. Similar to TNBC, HCC is characterized by high expression of PD-L1[15, 16] so that a cistron constructed by human telomerase reverse transcriptase (hTERT) promoter and αCD3HAC coding sequence is loaded on the CRAd to improve the old targeting system. In this study, the novel system will be investigated on synergistic anti-tumor effect and overcoming AFP heterogeneity.

Materials And Methods

Cell lines and cell culture

Human hepatoma cell lines (HepG2 and SMMC-7721), embryonic renal cell line 293 A and human embryonic kidney cell-derived 293T cell line (Institute of Hematology and Blood Diseases Hospital Chinese Academy of Medical Sciences and Peking Union Medical College, PUMC, Tianjin, China), were maintained in DMEM (#1791922, Gibco) supplemented with 10% FBS. Human T cell leukemia cell line Jurkat (Institute of Hematology and Blood Diseases Hospital Chinese Academy of Medical Sciences and Peking Union Medical College, PUMC, Tianjin, China) was maintained in RPMI 1640 (#1721503, Gibco) plus 10% FBS.

Preparation of adenoviruses

The constructions of adenoviruses were based on the AdEasy™ adenoviral vector system (#240009, Stratagene) and shown as Fig. 1A. The plasmid pAdTrack and pAdE1A had been established previously

[6]. And then, the tandem sequence of hTERT promoter and αCD3HAC was inserted into pAdTrack and pAdE1A respectively at the sites of *Kpn*I and *Bgl*II. Later, all the 4 shuttle vectors (pAdTrack, pAdE1A, pAdαCD3HAC, pAdE1A-αCD3HAC) were packaged using methods as described previously [6]. Adenoviral stocks were generated with a Vivapure AdenoPACK 20 kit (#VS-AVPQ020, Sartorius), and the titers were determined by 50% tissue culture infectious dose (TCID50).

Isolation, culture, and hepatic differentiation of HUMSC

HUMSCs were isolated from the gelatinous Wharton's jelly (WJ) within human umbilical cord and cultured using methods as described previously [14,17]. Induction of HUMSCs into hepatocyte-like cells was performed. Cells were seeded at a density of 1×10^4 cells/cm^2. At first, cells were treated with DMEM supplemented with 5% FBS, 20 ng/mL hepatocyte growth factor (HGF; # 294-HG-005, R&D), 10 ng/mL basic fibroblast growth factor (bFGF; #3718-FB-010, R&D), oncostatin M (OSM; #295-OM-010, R&D), 0.61 mg/mL nicotinamide (#N0636, Sigma), and 10^{-7}M dexamethasone (#D4902, Sigma) for a week. For the following days, cells were cultured in DMEM containing 5% FBS, 20 ng/mL HGF, 10 ng/mL bFGF, OSM, 0.61 mg/mL nicotinamide, 10^{-7}M dexamethasone, and 10% 100 × insulin-transferrin-selenium+1 liquid media supplement (#I3146, Sigma). The medium was changed twice in a week.

Luciferase assay for AFP promoter and hTERT promoter *in vitro*

pGL3-AFP promoter and pGL3-hTERT promoter had been constructed previously, and the transcriptional activities in HepG2 and SMMC-7721 were also detected using Dual-luciferase® reporter assay (#E1910, Promega) as described previously [6,18].

Isolation and culture of Peripheral blood mononuclear cells (PBMCs)

Blood of healthy donor was obtained from Tianjin Blood Center. PBMCs were isolated by Ficoll solution (#LTS10771, TBD Science). Cells were maintained in RPMI1640 plus 10% FBS and cultured in the presence of recombinant human IL-2 (100 U/mL; #202-IL-010, R&D) every other day.

CCK-8 assay

Cell viability assay for cytotoxicity of CRAd was detected by CCK-8 kit (#CK04, Dojindo). Cells were seeded in a 96-well plate at the density of 1×10^4 cells/well, and infected with different adenoviruses at 10, 50, or 100 MOI, respectively. Then, the cell viabilities were evaluated every 24 hours, from day 2 to day 4. The cells without infection were used as negative control. Each data point was averaged from three replicates of three separate experiments.

Establishment of PD-L1 overexpressed cell line

The sequences of human PD-L1 and firefly luciferase were linked by T2A sequence, and the linked sequence was inserted into pCDH1-CMV-MSC-EF1α-Puro plasmid (#CD510B, SBI) using *EcoR*I and

*BamH*I restriction sites. The lentivirus was packaged as described previously [19]. SMMC-7721 cells were transduced with the lentivirus for 48 h and selected with 30 μg/ml puromycin (#P8230; Beijing Solarbio Science & Technology) for 2 weeks. The new cell line was termed 7721-PD-L1.

Establishment of HepG2 with luciferase reporter

The sequence of firefly luciferase was inserted into pCDH1-CMV-MSC-EF1α-Puro plasmid using *EcoR*I and *BamH*I restriction sites. The lentivirus was packaged and infected to HepG2 cell as described above. After selection by 30 μg/ml puromycin, the stable cell line was established and termed HepG2-luc.

ELISA assay for αCD3HAC

HepG2 or SMMC-7721 was infected by the different adenoviruses at 50 MOI respectively for 48 hours, the culture supernatants were collected and the concentrations of αCD3HAC were measured using His Tag ELISA Detection Kit (#L00436, GenScript). Similarly, the concentrations of αCD3HAC in the supernatants of HepG2 or SMMC-7721 were measured as the same method everyday after infection with AdE1A-αCD3HAC. The assays were done in three replicates of three separate experiments.

αCD3HAC binding detection

SMMC-7721 cells were infected with the different adenoviruses respectively for 96 hours, then the culture supernatants were collected for detecting binding activity to PD-L1 of αCD3HAC by flow cytometry (FACS) on 7721-PD-L1 cell. For direct binding assay, 1×10^5 cells were suspended in 100 μL collected supernatant and added into 5 μL APC-His tag antibody (#362605, Biolegend). Cells without any supernatant were used as negative control, and cells with APC-human PD-L1 antibody (#374514, Biolegend) were used as positive control. After cultured at room temperature for 30 min, the cells were detected by FACS. For competition assay, 5 uL APC-human PD-L1 antibody was added into 7721-PD-L1 suspension of collected supernatant. Cells with APC-isotype control (#982108, Biolegend) were used as negative control, and cells only with APC-human PD-L1 antibody were used as positive control. FACS was performed after culturing. The binding assays to CD3 were manipulated like those above except replacing APC-human PD-L1 antibody into APC-human CD3 antibody (#300312, Biolegend).

Cytotoxicity and activation of T cell

The culture supernatants of SMMC-7721 infected with different adenoviruses were still used in the following experiments. 7721-PD-L1 cells were seeded into 96-well plates (1×10^4 cells/well). The next day, PBMCs pretreated with IL-2 for 72 hours were added at the effector: target (E: T) ratios of 5:1. And 100 uL supernatant was added simultaneously. 16 hours later, the specific cytotoxicity toward 7721-PD-L1 cells was measured by lactate dehydrogenase assay using the CytoTox 96 nonradioactive cytotoxicity kit (#G1780, Promega) according to the manufacturer's instructions. And then the cells and the culture supernatant of every well were separated. The cells were stained with APC- human CD3 antibody (#300312, Biolegend) and PE-human CD69 antibody (#310906, Biolegend) for 30 min at room

temperature and measured using FACS to detect activated T cells. The concentrations of IL-2, IFN-g and TNF-α in the supernatants were measured by the corresponding ELISA kits (D2050, DIF50C, DTA00D, R&D).

Jurkat apoptosis assay

7721-PD-L1 cell and Jurkat cell were cocultured in the supernatants collected previously at the ratio of 10:1 for 24 hours. Then the cells were separated and stained with APC-human CD3 antibody (#300312, Biolegend) and FITC-Annexin V (#556547, BD). The apoptosis of Jurkat cell was measured by FASC.

Adenovirus package in hepatic differentiated HUMSCs

HUMSCs were induced to hepatic differentiation for 10 days, then were infected with different adenoviruses at 500 MOI. The infected HUMSCs were separated at the indicated time and the copy numbers of virus DNA in these cells were measured by real-time PCR as described previously [18]. The collected HUMSCs at the 48 hours after infection with AdE1A or AdE1A-αCD3HAC were observed using electron microscope to find the adenovirus particles in them. On the other hand, 50 μL of supernatant removed from the hepatic differentiated HUMSCs infected with different adenoviruses was cocultured with HepG2 in 96-well plates at a density of 2500 cells/well, and after 2 days the HepG2 cells were observed using fluorescence microscope to confirm whether there were adenovirus particles in the supernatants.

Transwell migration assay

The migratory ability of infected HUMSCs was determined using cell culture inserts (#353097, BD Falcon) which were 6.5mmin diameter with 8 μm pore filters. HUMSCs were infected with the indicated adenovirus at 500 MOI for 48 hours and plated at a density of 2×10^4 in the top chamber with 200 μL of serum-free medium. And then the method was performed as described previously [6].

Orthotopic hepatocarcinoma model

The orthotopic hepatocarcinoma model was established with HepG2-luc or 7721-PD-L1 cell line on Balb/c athymic nude mouse. Briefly, 1×10^7 cells were injected subcutaneously into the right anterior flank of mouse. After 2 weeks, when the tumor reached to approximately 1 cm in diameter, it was isolated and cut into small pieces of equal volume (1 mm^3). And then Balb/c athymic nude mice were anesthetized and laparotomy was performed. After preparation of the liver, the right liver lobes were punctured to form about a 3-mm-long sinus tract and the fragment of tumor tissue was inserted into the sinus tract. Thus, the orthotopic hepatocarcinoma model was established. For AFP heterogeneous hepatocarcinoma model, HepG2 and 7721-PD-L1 cells were mixed at the ratio of 3:1, and then 2×10^7 cells were injected subcutaneously into the right anterior flank of mouse. Subsequently, the same operation proceeded as the orthotopic model.

Treatment of orthotopic hepatocarcinoma model

After 10 days of orthotopic tumor inoculation, mice were randomized into 3 or 5 groups (5 mice for each group) according requirement. After infected with the indicated adenovirus at 500 MOI for 48 hours, the HUMSCs were injected into each mouse (iv, 1×10^6 cells) on the 1^{st} and 4^{th} day. And then PBMCs were injected (iv, 6×10^6 cells/ mouse) at the 7^{th} and 10^{th} day. *In vivo* luciferase signal was monitored via Xenogen IVIS imaging at the indicated time points. Body weight was recorded twice a week after HUMSCs injection. on the 18^{th} day after treatment, mice were sacrificed and the serum levels of alanine aminotransferase (ALT) and aspartate transaminase (AST) were assessed using detection kits (#C009-2-1 and #C010-2-1, Nanjing Jiancheng Bioengineering Institute). At the same time, the tissues of tumor and some extrahepatic organs including lung, kidney and spleen were removed from model mice. The total RNA of tumor tissue was extracted using TRIzol reagent (#15596026, Invitrogen) and the quantitative RT-PCR was performed to detect the expression of PD-L1 gene as described previously [19]. The extrahepatic organs were fixed in 4% PFA, embedded in paraffin, sectioned, and stained with Hematoxylin–eosin (HE).

Immunofluorescence

To explore the adenovirus delivery by HUMSC, the tumor tissues of orthotopic hepatocarcinoma models treated by adenovirus armed HUMSC for 4 days were made into paraffin sections for immunofluorescence. The sections were stained with mouse anti-Hexon primary antibody (#GTX36896, GeneTex) and AF488-conjugated goat anti-mouse secondary antibody (#ab150113, Abcam) to detect the adenovirus hexon protein. Meanwhile, rabbit anti-human CD90 primary antibody (#ab 226123, Abcam) and AF647-conjugated goat anti-rabbit secondary antibody (#ab150079, Abcam) were used to indicate HUMSCs. Nuclei were stained with DAPI (#D9564, Sigma). Images were captured by a two-photon laser scanning confocal microscope (FV1200 MPE, OLYMPUS). Similarly, the tumor tissues of model mice treated by HUMSC.Ad and PBMC for 16 days were prepared for paraffin sections, and then stained with mouse anti-Hexon primary antibody, AF488-conjugated goat anti-mouse secondary antibody, rabbit anti-His tag primary antibody (#ab213204, Abcam) and AF647-conjugated goat anti-rabbit secondary antibody to indicate hexon and αCD3HAC.

FACS for T cells in tumor

After model mice were treated by HUMSC.Ad+PBMC for 16 days, the tumors were cut into approximately 1 mm^3 pieces and digested with 0.05 mg/mL of type-IV collagenase (#C5138, Sigma), hyaluronidase (#H3506, Sigma) and DNase I (D5025, Sigma) at 37°C for 60 min. Single cells were obtained by grinding through a 70 μm strainer. Subsequently, mononuclear cells were obtained by density gradient centrifugation using 40% percoll and 80% percoll (#17-0891-09, GE). And then cells were stained with APC-human CD3 antibody and PE-human CD69 antibody. FACS were used to detect the activated T cells.

Coculture and killing assay

HepG2 cells were seeded in 24 well plate at the density of 5×10^4 cells/well and infected with different adenoviruses at 50 MOI for 24 hours. And then, the infected HepG2 cells and 7721-PD-L1 cells were used to established coculture system. 5×10^4 7721-PD-L1 cells were seeded in lower chamber of 24-well plate, and 2×10^4 infected HepG2 cells were seeded in upper chamber with 0.4 μm pore filters (#353095, BD Falcon). 48 hours later, the upper chamber was removed and 1×10^6 PBMCs were added into culture medium for 24 hours. Lastly, culture medium and suspended cells were removed and 500 μL/well of D-luciferin (0.15mg/mL, Promega, USA) was added. Bioluminescence imaging was performed immediately using IVIS-Xenogen 100 system.

Statistical analysis

The data were analyzed using independent sample *t* tests and represented as mean±SD. $p<0.05$ was considered to be statistically significant and $p<0.01$ was considered to be highly statistically significant.

Results

Function identification of CRAd Loaded with αCD3HAC

The CRAds were constructed as shown in Fig.1A. One of them, designated as AdE1A, had been used in the old targeting system. AdE1A-αCD3HAC was the improved one with the αCD3HAC expression cassette. And then, two HCC cell lines were selected as experimental objects with the different AFP expression levels, HepG2 was the positive one and SMMC-7721 was the negative (Fig. S1A). Subsequently, the transcriptional activities of AFP promoter and hTERT promoter were detected in these two cell lines. The activity of AFP promoter was significantly higher in HepG2 than in SMMC-7721, and the activity of TERT promoter was similar in both of them (Fig. 1B). Predictably, the survivals of HepG2 were dramatically decreased by AdE1A and AdE1A-αCD3HAC in a dose-dependent manner, because of the presence of E1A expression unit controlled by AFP promoter and miR-122 target sequence. The cell inhibitory effect of AdE1A-αCD3HAC was similar to which of AdE1A at the same MOI. However, the 4 adenoviruses, whether with or without E1A expression unit, all did not affect the survivals of SMMC-7721 (Fig. 1C). Furthermore, the expression of αCD3HAC driven by hTERT promoter was observed in HepG2 cells infected with AdαCD3HAC or AdE1A-αCD3HAC (Fig. S1B). Likewise, the αCD3HACs secreted from HepG2 and SMMC-7721 infected with AdE1A or AdE1A-αCD3HAC were all detectable obviously in the culture supernatants (Fig. 1D). Lastly, variations of αCD3HAC level in supernatants from 24 hours to 96 hours after infection with AdE1A-αCD3HAC were investigated. In SMMC-7721 supernatant, the concentration of αCD3HAC was maintain a continuous upward trend during 96 hours. But in HepG2 supernatant, owing to the cell death resulting from cytolytic effect of CRAd, the concentration of αCD3HAC did not increase remarkblely at 96 hours after infection (Fig. 1E).

Function identification of αCD3HAC secreted from infected cell

For determining the binding activity of αCD3HAC to PD-L1, SMMC-7721 overexpressed human PD-L1 (7721-PD-L1), was established firstly. And then the supernatants of SMMC-7721 infected with the

different adenoviruses respectively for 96 hours were collected for the following experiments. In the direct binding and competition assays, it was verified that the αCD3HACs in the supernatants of SMMC-7721 infected with AdαCD3HAC or AdE1A-αCD3HAC could bind to 7721-PD-L1 and compete with the purchased PD-L1 antibody (Fig. 2A and 2B). Similarly, αCD3HAC in supernatant also could bind to Jurkat, a CD3 positive cell line, and compete with purchased CD3 antibody (Fig. 2C and 2D). Comparing to the competitive ability of αCD3HAC to CD3, which to PD-L1 was less remarkable. The reason was that the binding sites of αCD3HAC and purchased antibody were different on PD-L1, but same on CD3. After 7721-PD-L1 (target cell) and PBMC (effect cell) were cocultured with medium containing the indicated supernatants respectively for 24 hours more than 60% of target cells were eliminated by effect cells in the medium containing αCD3HAC (Fig. 2E); and the proportions of CD69 positive (activated) T cells were also increased to about 90% by αCD3HAC (Fig. 2F and S2). As the products of activated T cells, IL-2, IFN-g and TNF-α in coculture medium containing αCD3HAC were also apparently increased (Fig. 2G-I). PD-L1 could induce apoptosis of PD-1 positive cells including T cell. Therefore, the apoptosis of Juarkat (PD-1 positive) induced by 7721-PD-L1 with the collected supernatant respectively was determined. The result showed that αCD3HAC exactly inhibited the apoptosis induced by PD-L1 (Fig. 2J and S3)

Package and delivery of adenovirus by HUMSC

After be induced hepatic differentiation for 10 days *in vitro*, HUMSCs were loaded with different adenoviruses respectively. And then these HUMSCs were collected every day to measure the copies of viral DNA in them for 3 days. The curves in Fig. 3A demonstrated that the content of adenovirus in differentiated HUMSC peaked at 48 hours after infection with AdE1A or AdE1A-αCD3HAC, but no viral DNA was detected in the HUMSCs infected with other adenoviruses. Under electron microscope, adenovirus particles were discovered in differentiated HUMSC infected with AdE1A or AdE1A-αCD3HAC (Fig. 3B). To verify that the packaged adenovirus could be released from the HUMSCs, the supernatants of differentiated HUMSCs loaded with the adenoviruses respectively were added onto HepG2 cells. After 2 days, HepG2 cells with supernatant from MSC.AdE1A or MSC.AdE1A-αCD3HAC showed clustered green fluorescence, because the corresponding adenoviruses were released into supernatants from differentiated HUMSCs and propagated in the AFP positive cells after infecting them, but cells with supernatant from MSC.AdTrack or MSC.AdαCD3HAC did not (Fig. 3C). On the other hand, it was demonstrated by transwell assay that the migration capability of HUMSC had not been affected by loading with adenovirus (Fig. S4). For investigating the delivery of adenvovirus by HUMSC *in vivo*, MSC.ads were intravenously injected into orthotopic hepatocarcinoma model mice. Four days later, the tumor tissues were removed and observed under confocal microscope. In the tissues form mice treated by MSC.AdTrack or MSC.AdαCD3HAC, it was found that there were scattered HUMSCs marked by CD90-antibody (Red). However, HUMSCs were disappeared in the tissues form mice treated by MSC.AdE1A or MSC.AdE1A-αCD3HAC and replaced by clustered adenoviruses stained with hexon-antibody (Green) (Fig. 3D). It was indicated that MSC.ads could home into tumor tissue, and which of them loaded with adenovirus containing AFP promoter-E1A element were lysed and released the adenovirus when they differentiated.

Inhibitory effect against orthotopic liver xenograft tumor

To explore the tumor inhibitory effect of the new improved targeting system, orthotopic hepatocarcinoma model mice were established using HepG2-luc and the administration of MSC.Ad and PBMC was shown as Fig. 4A. After 8 days of treatment, the tumors were inhibited significantly by MSC.AdE1A or MSC.AdE1A-αCD3HAC, but there was no remarkable difference between these two treatment groups. Subsequently，on the 16^{th} day after treatment, the tumors of MSC.AdE1A+PBMC or MSC.AdE1A-αCD3HAC+PBMC groups were still smaller than which of other groups. From the 8^{th} day to the 16^{th}, it was noteworthy that the treatment of MSC.AdE1A-αCD3HAC+PBMC got better tumor inhibitory effect than MSC.AdE1A+PBMC because of the anti-tumor function of PBMC mediated by αCD3HAC (Fig. 4B, 4C and S5). To evaluate the liver injuries of these model mice under the different therapy strategies, ALT and AST in serum were detected. As shown in Fig. 4D, the levels of ALT and AST were all declined by treating with MSC.AdE1A+PBMC or MSC.AdE1A-αCD3HAC+PBMC; the ALT levels exhibited remarkable different between these two groups but the AST levels did not. Additionally, no marked difference was found in weight change and pathologic feature of extrahepatic organs among the all treatment groups (Fig. S6). Adenovirus and INF-g could promote PD-L1 expression so that the PD-L1 in tumor was measured by quantitative PCR. Just as we expect, the levels of PD-L1 in tumors of MSC.AdE1A+PBMC and MSC.AdE1A-αCD3HAC+PBMC treatment groups were elevated obviously. Although the PD-L1 positive cell was the target of T cell mediated by αCD3HAC, no significant difference was found in PD-L1 expression level between these two groups (Fig. 4E).

Expression of αCD3HAC and activation of T cell in tumor tissue

To verify the expression of αCD3HAC in tumor tissue, confocal microscope was performed. On the tumor tissue sections of MSC.AdE1A-αCD3HAC+PBMC treatment group， adenovirus hexon protein (Green) and αCD3HAC (Red) were both found and their distributions were similar. Only hexon but no αCD3HAC was shown on the sections of MSC.AdE1A+PBMC group, and there was neither hexon nor αCD3HAC in the tumors of the other groups (Fig. 5A). Infection and proliferation of adenoviruses in tumor could promote T lymphocytes infiltration and αCD3HAC could maintain their survival by activating them directly and blocking PD-L1 to avoid them from apoptosis. Therefore, lymphocytes in tumor were isolated and the proportion of activated T cell was measured by FACS. Few CD3 positive T cells were found in the tumors of MSC.AdTrack+PBMC and MSC.AdαCD3HAC+PBMC groups (Fig. S7), but in the tumors of MSC.AdE1A+PBMC and MSC.AdE1A-αCD3HAC+PBMC groups, the infiltration of T cells increased significantly (Fig. 5B). Moreover, the proportions of not only total T cells, but also activated T cells in the tumors of MSC.AdαCD3HAC+PBMC group were higher than which of MSC.AdE1A+PBMC group (Fig. 5B-D).

Inhibitory effect on AFP heterogeneous hepatocarcinoma model

Previously, it had been identified that both AdE1A and AdE1A-αCD3HAC could not make SMMC-7721 cell lysis *in vitro* (Fig. 1C). Here, the treatment effects of MSC.AdE1A+PBMC and MSC.AdE1A-

αCD3HAC+PBMC on 7721-PD-L1 orthotopic liver xenograft model mice were further considered. Although αCD3HAC could be released by 7721-PD-L1 infected with AdE1A-αCD3HAC, the treatments of MSC.AdE1A+PBMC and MSC.AdE1A-αCD3HAC+PBMC had not inhibited the tumor growth (Fig.S8). It was speculated that there was not enough αCD3HAC to evoke the anti-tumor effect of T lymphocytes in the unitary AFP negative tumor model. If tumor tissue contained both AFP positive and negative cells, amounts of αCD3HAC would be supported by the replication of AdE1A-αCD3HAC in AFP positive cells to facilitate the clearance of the AFP negative ones. In order to test this assumption, a coculture experiment was performed as Fig. 6A. The result demonstrated that the killing effect against 7721-PD-L1 mediated by HepG2 with AdE1A-αCD3HAC was more significant than which mediated by HepG2 with AdαCD3HAC (Fig 6B and C), because the released adenovirus was spread into lower chamber through the membrane with 0.4 mm pore and infected the 7721-PD-L1 subsequently to sustained higher concentration of αCD3HAC in the supernatant. And then the treatment of MSC.AdE1A-αCD3HAC+PBMC was evaluated on the AFP heterogeneous tumor model. Comparing to the untreated and the MSC.AdE1A+PBMC treated groups, the signal of 7721-PD-L1 was remarkably decreased in the MSC.AdE1A-αCD3HAC+PBMC treated group (Fig. 6D-E and S9). This result indicated that MSC.AdE1A-αCD3HAC+PBMC would be used to overcome the problem resulted from AFP heterogeneity.

Discussion

Since we had found that the AFP promoter would be activated during the hepatic differentiation of HUMSC, the HUMSCs were used as *in vivo* delivery vehicle of CRAds or therapeutic proteins controlled by AFP promoter against HCC [6, 18, 20, 21]. In terms of CRAd, AFP promoter was also a regulator for its specific replication in tumor cells, and miR-122 target sequence was another regulator for further reducing side effect to normal hepatocytes [6]. Although this CRAd delivered by HUMSC had exhibited better antitumor effect and safety, it still needs to be improved for two reasons: 1) The tumor inhibition rate was unsatisfactory so that combination with other antitumor method would be necessary; 2) The intratumoral heterogeneous expression of AFP was an important feature of HCC [22, 23], hence the selectivity of the CRAd only to AFP positive cell would result in failure to eliminate tumor completely.

Nowadays, many BiTEs had been armed on CRAds to play a synergistic anti-tumor effect [24–26]. In this study, we had established a novel CRAd (AdE1A-αCD3HAC) with a PD-L1 targeting BiTE (αCD3HAC), which had been applied in the treatment for TNBC by us previously [14]. In the sequence of αCD3HAC, the part of anti-CD3 scFv was cloned from the variable region of an IgG antibody (HIT3a) and the part of HAC was a mutant of PD-1 ectodomain with high affinity to PD-L1 [27]. The expression of αCD3HAC was under the control of hTERT promoter, a popular tumor specific promoter, which would guarantee the release of αCD3HAC from both AFP positive cell and the negative after infection. After a series of identification experiments including selective killing activity of CRAd, release and binding activity of αCD3HAC and T cell activation mediated by αCD3HAC, it had been confirmed that the characters of AdE1A-αCD3HAC were consistent to our expectation.

Although it had been validated that AdE1A could be delivered and packaged by HUMSC in our previous paper [6], the same validation experiments still need to be performed on AdE1A-αCD3HAC because loading αCD3HAC on it would maybe interfere adenovirus packaging. Experiments *in vitro* had showed that AdE1A-αCD3HAC was similar to AdE1A in respects of adenovirus package and HUMSC migration when be loaded on HUMSC. The delivery of adenovirus by HUMSC was also discovered on tumor tissue sections of the orthotopic xenograft model mice. At the appropriate time point, CRAds could be observed in tumor tissues of MSC.AdE1A and MSC.AdE1A-αCD3HAC treatment groups, whereas there were only HUMSCs but not CRAds in tumor tissues of MSC.AdTrack and MSC.AdαCD3HAC treatment groups because of the absence of E1A driven by AFP promoter. It was indicated that, like AdE1A, AdE1A-αCD3HAC was exactly delivered and released by HUMSC *in vivo*.

The expression of PD-L1 was high in HCC and would be increased after stimulation by virus and IFN-γ [28–31]. The existence of large amount of PD-L1 in tumor would not be beneficial to the survival of effect lymphocytes. The reason of choosing αCD3HAC to enhance anti-tumor effect was that it did not only block PD-L1 to make T cell survival, but also active them for proliferation and specific killing. Through the detection of lymphocytes isolated from tumor tissues of orthotopic xenograft model mice by FACS, it was verified that αCD3HAC increased the proportion of intratumoral T cells and made them active. Therefore, sequential therapy of MSC.AdE1A-αCD3HAC + PBMCs had better anti-tumor effect than MSC.AdE1A + PBMCs on orthotopic hepatocarcinoma models. Before PBMCs came into play, MSC.AdE1A-αCD3HAC and MSC.AdE1A had got similar inhibition rates. Along with the participation of PBMCs, the function of αCD3HAC had been exhibited, which resulted in the further increase of tumor inhibition rate of MSC.AdαCD3HAC + PBMC group. After treatment, we discovered that PD-L1 levels in tumor tissues from MSC.AdE1A-αCD3HAC + PBMCs and MSC.AdE1A + PBMCs groups were remarkably higher than which from other groups. In spite of that αCD3HAC had mediated the specific lysis of PD-L1 positive cell, the total PD-L1 level of tumor tissue from MSC.AdE1A-αCD3HAC + PBMCs treatment group did not decline significantly. This result hinted that the function of αCD3HAC would not disappear in a short time when the model mice were treated by MSC.AdαCD3HAC + PBMC.

Importantly, many mechanisms were designed in the new system to avoid side effect: 1) homing and hepatic differentiation of HUMSC controlled the release of CRAds only in the tumor tissue; (2) AFP promoter and miR-122 target sequence ensured the selectivity to tumor cell; (3) hTERT promoter was active in tumor cell but inactive in HUMSC [18] so that the distribution of αCD3HAC was limited in local tumor site. According to the above designs, the treatment of MSC.AdE1A-αCD3HAC + PBMC had not affected the body weight and extrahepatic organs. As biomarkers of liver injury, serum ALT and AST had declined in model mice of MSC.AdE1A-αCD3HAC + PBMC and MSC.AdE1A + PBMC treatment groups. Comparing to MSC.AdE1A + PBMC group, MSC.AdE1A-αCD3HAC + PBMC group had shown lower level of ALT. It illustrated that MSC.AdE1A-αCD3HAC + PBMC not only alleviated the injury of normal hepatocytes caused by tumor, but also did not have more significant live side effect than MSC.AdE1A + PBMC.

Like to other solid tumors, immunotherapy to HCC had to face to many problems, such as effective and safe targeting, infiltration and survival of lymphocytes, tumor heterogeneity and immunosuppressive

microenvironment [33, 34]. Through the above studies, it could be concluded that the new targeting system had solved the first two problems in a large extent. In the old system, the recognition of tumor cell did mainly depend on AFP promoter, and therefore the heterogeneous expression of AFP in tumor would definitely limit its anti-tumor effect. αCD3HAC at local tumor site could re-target tumor cell by PD-L1, so that the treatment of MSC.AdαCD3HAC + PBMC had showed notable killing capacity to AFP negative tumor cell on AFP heterogeneous model mice. Theoretically, there were many mechanisms by which AdE1A-αCD3HAC would overcome the problem of tumor microenvironment [34–36]: 1) oncolytic virus could convert “cold” microenvironment to “hot”; 2) αCD3HAC could represent a general means of T-cell rejuvenation for durable cancer immunotherapy, owing to targeting PD-L1 on dendritic cells; 3) oncolytic virus promoted the antigen-presentation by pathogen-associated molecular patterns (PAMPs). Additionally, the activation of $CD4^+$ T cell by αCD3HAC and the neo-antigens released from lytic tumor cells would synergistically evoke specific anti-tumor immune response, which was also an effective method to solve the problem of heterogeneity. However, because the tumor xenograft models in this study were established using Balb/c athymic nude mouse, the influence of αCD3HAC on tumor microenvironment had not been exhibited sufficiently. Therefore, the change of tumor microenvironment caused by CRAd and αCD3HAC should be further discussed on humanized mice in our future work.

Conclusions

A BiTE, αCD3HAC, driven by hTERT promoter was loaded on CRAd of the old HCC targeting system to overcome the limitation caused by the selectivity to AFP positive cell and strengthen the anti-tumor effect. In the new system, the homing and hepatic differentiation of HUMSC, the package of CRAd and the release of αCD3HAC were all not affected by the participation of αCD3HAC expression cassettes. The new system exhibited a better anti-tumor effect with no more damage to extrahepatic organs and less liver injury, comparing the old one. The αCD3HAC released from the AFP positive cells re-targeted the PD-L1 positive cells to facilitate the elimination of AFP negative cells in AFP heterogeneous tumor model. Taken together, the new system would provide a more effective and safer strategy against HCC.

Declarations

Ethics approval and consent to participate

All animal studies were performed in accordance with guidelines under the Animal Ethics Committee of Tianjin NanKai Hospital.

Consent for publication

Not applicable.

Availability of data and materials

The dataset supporting the conclusions of this article is included within the article.

Competing interests

The authors declare that they have no competing interests.

Funding

This work was supported by the Tianjin Municipal Science and Technology Commission Grant (Grant Nos. 19JCZDJC33100), the National Natural Science Foundation of China (Grant Nos. 82003266, 81830005)

Authors' contributions

XY wrote the main manuscript text, designed and performed the all experiments. YL constructed the adenoviruses, established stable expression cell line and participated animal operation. YY prepared all figures, performed electron microscope assay and participated animal operation. WT contributed to the HE staining and confocal microscopic Imaging. DF participated the isolation of PBMCs and HUMSCs. RL contributed to the FACS assay. XL performed western blotting and luciferase assays. YX contributed to the ELISA assays. LY contributed to the cytotoxicity experiments. SY and DX were the corresponding authors, participated the design of this subject and revised this paper. All authors read and approved the final manuscript.

Acknowledgements

Not applicable.

References

1. Ju Dong Yang, Pierre Hainaut, Gregory J Gores, Amina Amadou, Amelie Plymoth, Lewis R Roberts. A global view of hepatocellular carcinoma: trends, risk, prevention and management. Nat Rev Gastroenterol Hepatol. 2019;16(10):589–604.
2. Tim F Greten, Chunwei Walter Lai, Guangfu Li, Kevin F Staveley-O'Carroll. Targeted and Immune-Based Therapies for Hepatocellular Carcinoma. Gastroenterology. 2019;156(2):510–524.
3. Benjamin Ruf, Bernd Heinrich, Tim F Greten. Immunobiology and immunotherapy of HCC: spotlight on innate and innate-like immune cells. Cell Mol Immunol. 2021 Jan;18(1):112–127.
4. David J Pinato, Nadia Guerra, Petros Fessas, Ravindhi Murphy, Takashi Mineo, Francesco A Mauri, Sujit K Mukherjee, Mark Thursz, Ching Ngar Wong, Rohini Sharma, Lorenza Rimassa. Immune-based therapies for hepatocellular carcinoma. Oncogene. 2020;39(18):3620–3637.
5. Morteza Hafezi, Meiyin Lin, Adeline Chia, Alicia Chua, Zi Zong Ho, Royce Fam, Damien Tan, Joey Aw, Andrea Pavesi, Thinesh Lee Krishnamoorthy, Wan Cheng Chow, Wenjie Chen, Qi Zhang, Lu-En Wai, Sarene Koh, Anthony T Tan, Antonio Bertoletti. Immunosuppressive Drug-Resistant Armored T-Cell Receptor T Cells for Immune Therapy of HCC in Liver Transplant Patients. Hepatology. 2021;74(1):200–213.

6. Xiangfei Yuan, Qing Zhang, Zhenzhen Li, Xiaolong Zhang, Shiqi Bao, Dongmei Fan, Yongxin Ru, Shuxu Dong, Yizhi Zhang, Yanjun Zhang, Zhou Ye, Dongsheng Xiong. Mesenchymal stem cells deliver and release conditionally replicative adenovirus depending on hepatic differentiation to eliminate hepatocellular carcinoma cells specifically. Cancer Lett. 2016;381(1):85–95.
7. Claudia Manuela Arnone, Vinicia Assunta Polito, Angela Mastronuzzi, Andrea Carai, Francesca Camassei Diomedi, Laura Antonucci, Lucia Lisa Petrilli, Maria Vinci, Francesco Ferrari, Elisa Salviato, Marco Scarsella, Cristiano De Stefanis, Gerrit Weber, Concetta Quintarelli, Biagio De Angelis, Malcolm K Brenner, Stephen Gottschalk, Valentina Hoyos, Franco Locatelli, Ignazio Caruana, Francesca Del Bufalo. Oncolytic adenovirus and gene therapy with EphA2-BiTE for the treatment of pediatric high-grade gliomas. J Immunother Cancer. 2021;9(5):e001930.
8. Johannes P W Heidbuechel, Christine E Engeland. Oncolytic viruses encoding bispecific T cell engagers: a blueprint for emerging immunovirotherapies. J Hematol Oncol. 2021;14(1):63.
9. Caroline E Porter, Amanda Rosewell Shaw, Youngrock Jung, Tiffany Yip, Patricia D Castro, Vlad C Sandulache, Andrew Sikora, Stephen Gottschalk, Michael M Ittman, Malcolm K Brenner, Masataka Suzuki. Oncolytic Adenovirus Armed with BiTE, Cytokine, and Checkpoint Inhibitor Enables CAR T Cells to Control the Growth of Heterogeneous Tumors. Mol Ther. 2020;28(5):1251–1262.
10. Shujie Zhou, Mingguo Liu, Fei Ren, Xiangjiao Meng, Jinming Yu. The landscape of bispecific T cell engager in cancer treatment. Biomark Res. 2021;9(1):38.
11. Alison Tedcastle, Sam Illingworth, Alice Brown, Leonard W Seymour, Kerry D Fisher. Actin-resistant DNAse I Expression From Oncolytic Adenovirus Enadenotucirev Enhances Its Intratumoral Spread and Reduces Tumor Growth. Mol Ther. 2016;24(4):796–804.
12. Zong Sheng Guo, Binfeng Lu, Zongbi Guo, Esther Giehl, Mathilde Feist, Enyong Dai, Weilin Liu, Walter J Storkus, Yukai He, Zuqiang Liu, David L Bartlett. Vaccinia virus-mediated cancer immunotherapy: cancer vaccines and oncolytics. J Immunother Cancer. 2019;7(1):6.
13. Yaomei Tian, Daoyuan Xie, Li Yang. Engineering strategies to enhance oncolytic viruses in cancer immunotherapy. Signal Transduct Target Ther. 2022;7(1):117.
14. Yuanyuan Yang, Xiaolong Zhang, Fangzhen Lin, Mengshang Xiong, Dongmei Fan, Xiangfei Yuan, Yang Lu, Yuewen Song, Yizi Zhang, Mu Hao, Zhou Ye, Yanjun Zhang, Jianxiang Wang, Dongsheng Xiong. Bispecific CD3-HAC carried by E1A-engineered mesenchymal stromal cells against metastatic breast cancer by blocking PD-L1 and activating T cells. J Hematol Oncol. 2019;12(1):46.
15. Hiroki Murai, Takahiro Kodama, Kazuki Maesaka, Shoichiro Tange, Daisuke Motooka, Yutaka Suzuki, Yasuyuki Shigematsu, Kentaro Inamura, Yoshihiro Mise, Akio Saiura, Yoshihiro Ono, Yu Takahashi, Yota Kawasaki, Satoshi Iino, Shogo Kobayashi, Masashi Idogawa, Takashi Tokino, Tomomi Hashidate-Yoshida, Hideo Shindou, Masanori Miyazaki, Yasuharu Imai, Satoshi Tanaka, Eiji Mita, Kazuyoshi Ohkawa, Hayato Hikita, Ryotaro Sakamori, Tomohide Tatsumi, Hidetoshi Eguchi, Eiichi Morii, Tetsuo Takehara. Multiomics identifies the link between intratumor steatosis and the exhausted tumor immune microenvironment in hepatocellular carcinoma. Hepatology. 2022 May 14. doi: 10.1002/hep.32573.

16. Alessandro Rizzo, Angela Dalia Ricci, Alessandro Di Federico, Giorgio Frega, Andrea Palloni, Simona Tavolari, Giovanni Brandi. Predictive Biomarkers for Checkpoint Inhibitor-Based Immunotherapy in Hepatocellular Carcinoma: Where Do We Stand? Front Oncol. 2021;11:803133.
17. Xiaolong Zhang, Yuanyuan Yang, Leisheng Zhang, Yang Lu, Qing Zhang, Dongmei Fan, Yizhi Zhang, Yanjun Zhang, Zhou Ye, Dongsheng Xiong. Mesenchymal stromal cells as vehicles of tetravalent bispecific Tandab (CD3/CD19) for the treatment of B cell lymphoma combined with IDO pathway inhibitor D-1-methyl-tryptophan. J Hematol Oncol. 2017;10(1):56.
18. Zhenzhen Li, Zhou Ye, Xiaolong Zhang, Qing Zhang, Dongmei Fan, Yanjun Zhang, Hongbo R Luo, Xiangfei Yuan, Zongfang Li, Dongsheng Xiong. E1A-engineered human umbilical cord mesenchymal stem cells as carriers and amplifiers for adenovirus suppress hepatocarcinoma in mice. Oncotarget. 2016;7(32):51815–51828.
19. Xiangfei Yuan, Wencong Tian, Yang Hua, Lijuan Hu, Jing Yang, Junmuzi Xie, Jiacai Hu, Feng Wang. Rhein enhances the cytotoxicity of effector lymphocytes in colon cancer under hypoxic conditions. Exp Ther Med. 2018;16(6):5350–5358.
20. Cihui Yan, Ming Yang, Zhenzhen Li, Shuangjing Li, Xiao Hu, Dongmei Fan, Yanjun Zhang, Jianxiang Wang, Dongsheng Xiong. Suppression of orthotopically implanted hepatocarcinoma in mice by umbilical cord-derived mesenchymal stem cells with sTRAIL gene expression driven by AFP promoter. Biomaterials. 2014;35(9):3035–43.
21. Qing Zhang, Xiangfei Yuan, Yang Lu, Zhenzhen Li, Shiqi Bao, Xiaolong Zhang, Yuanyuan Yang, Dongmei Fan, Yizhi Zhang, Chenxuan Wu, Hongxing Guo, Yanjun Zhang, Zhou Ye, Dongsheng Xiong. Surface expression of anti-CD3scfv stimulates locoregional immunotherapy against hepatocellular carcinoma depending on the E1A-engineered human umbilical cord mesenchymal stem cells. Int J Cancer. 2017;141(7):1445–1457.
22. Dirk Andreas Ridder, Arndt Weinmann, Mario Schindeldecker, Lana Louisa Urbansky, Kristina Berndt, Tiemo Sven Gerber, Hauke Lang, Johannes Lotz, Karl J Lackner, Wilfried Roth, Beate Katharina Straub. Comprehensive clinicopathologic study of alpha fetoprotein-expression in a large cohort of patients with hepatocellular carcinoma. Int J Cancer. 2022;150(6):1053–1066.
23. Juliane Friemel, Markus Rechsteiner, Lukas Frick, Friederike Böhm, Kirsten Struckmann, Michèle Egger, Holger Moch, Mathias Heikenwalder, Achim Weber. Intratumor heterogeneity in hepatocellular carcinoma. Clin Cancer Res. 2015;21(8):1951–61.
24. Johannes P W Heidbuechel, Christine E Engeland. Oncolytic viruses encoding bispecific T cell engagers: a blueprint for emerging immunovirotherapies. J Hematol Oncol. 2021;14(1):63.
25. Caroline E Porter, Amanda Rosewell Shaw, Youngrock Jung, Tiffany Yip, Patricia D Castro, Vlad C Sandulache, Andrew Sikora, Stephen Gottschalk, Michael M Ittman, Malcolm K Brenner, Masataka Suzuki. Oncolytic Adenovirus Armed with BiTE, Cytokine, and Checkpoint Inhibitor Enables CAR T Cells to Control the Growth of Heterogeneous Tumors. Mol Ther. 2020;28(5):1251–1262.
26. Jana de Sostoa, Carlos Alberto Fajardo, Rafael Moreno, Maria D Ramos, Martí Farrera-Sal, Ramon Alemany. Targeting the tumor stroma with an oncolytic adenovirus secreting a fibroblast activation

protein-targeted bispecific T-cell engager. J Immunother Cancer. 2019;7(1):19.

27. Roy L Maute, Sydney R Gordon, Aaron T Mayer, Melissa N McCracken, Arutselvan Natarajan, Nan Guo Ring, Richard Kimura, Jonathan M Tsai, Aashish Manglik, Andrew C Kruse, Sanjiv S Gambhir, Irving L Weissman, Aaron M Ring. Engineering high-affinity PD-1 variants for optimized immunotherapy and immuno-PET imaging. Proc Natl Acad Sci U S A. 2015;112(47):E6506-14.
28. asunao Numata, Noriyuki Akutsu, Keisuke Ishigami, Hideyuki Koide, Kohei Wagatsuma, Masayo Motoya, Shigeru Sasaki, Hiroshi Nakase. Synergistic effect of IFN-γ and IL-1β on PD-L1 expression in hepatocellular carcinoma. Biochem Biophys Rep. 2022;30:101270.
29. Naoki Okada, Ko Sugiyama, Shunsuke Shichi, Yasuhito Shirai, Kaoru Goto, Fumio Sakane, Hidemitsu Kitamura, Akinobu Taketomi. Combination therapy for hepatocellular carcinoma with diacylglycerol kinase alpha inhibition and anti-programmed cell death-1 ligand blockade. Cancer Immunol Immunother. 2022;71(4):889–903.
30. Peng Lv, Xiaomei Chen, Shiying Fu, En Ren, Chao Liu, Xuan Liu, Lai Jiang, Yun Zeng, Xiaoyong Wang, Gang Liu. Surface engineering of oncolytic adenovirus for a combination of immune checkpoint blockade and virotherapy. Biomater Sci. 2021;9(22):7392–7401.
31. Huan Zhang, Weimin Xie, Yuning Zhang, Xiwen Dong, Chao Liu, Jing Yi, Shun Zhang, Chunkai Wen, Li Zheng, Hua Wang. Oncolytic adenoviruses synergistically enhance anti-PD-L1 and anti-CTLA-4 immunotherapy by modulating the tumour microenvironment in a 4T1 orthotopic mouse model. Cancer Gene Ther. 2022;29(5):456–465.
32. Peter G Hendrickson, Michael Olson, Tim Luetkens, Siani Weston, Tiffany Han, Djordje Atanackovic, Gabriel C Fine. The promise of adoptive cellular immunotherapies in hepatocellular carcinoma. Oncoimmunology. 2019;9(1):1673129.
33. Jiaojiao Guo, Qi Tang. Recent updates on chimeric antigen receptor T cell therapy for hepatocellular carcinoma. Cancer Gene Ther. 2021;28(10–11):1075–1087.
34. Mengling Wu, Qianrui Huang, Yao Xie, Xuyi Wu, Hongbo Ma, Yiwen Zhang, Yong Xia. Improvement of the anticancer efficacy of PD-1/PD-L1 blockade via combination therapy and PD-L1 regulation. J Hematol Oncol. 2022;15(1):24.
35. Longchao Liu, Jiahui Chen, Joonbeom Bae, Huiyu Li, Zhichen Sun, Casey Moore, Eric Hsu, Chuanhui Han, Jian Qiao, Yang-Xin Fu. Rejuvenation of tumour-specific T cells through bispecific antibodies targeting PD-L1 on dendritic cells. Nat Biomed Eng. 2021;5(11):1261–1273.
36. Greyson Willis Grossman Biegert, Amanda Rosewell Shaw, Masataka Suzuki. Current development in adenoviral vectors for cancer immunotherapy. Mol Ther Oncolytics. 2021;23:571–581.

Figures

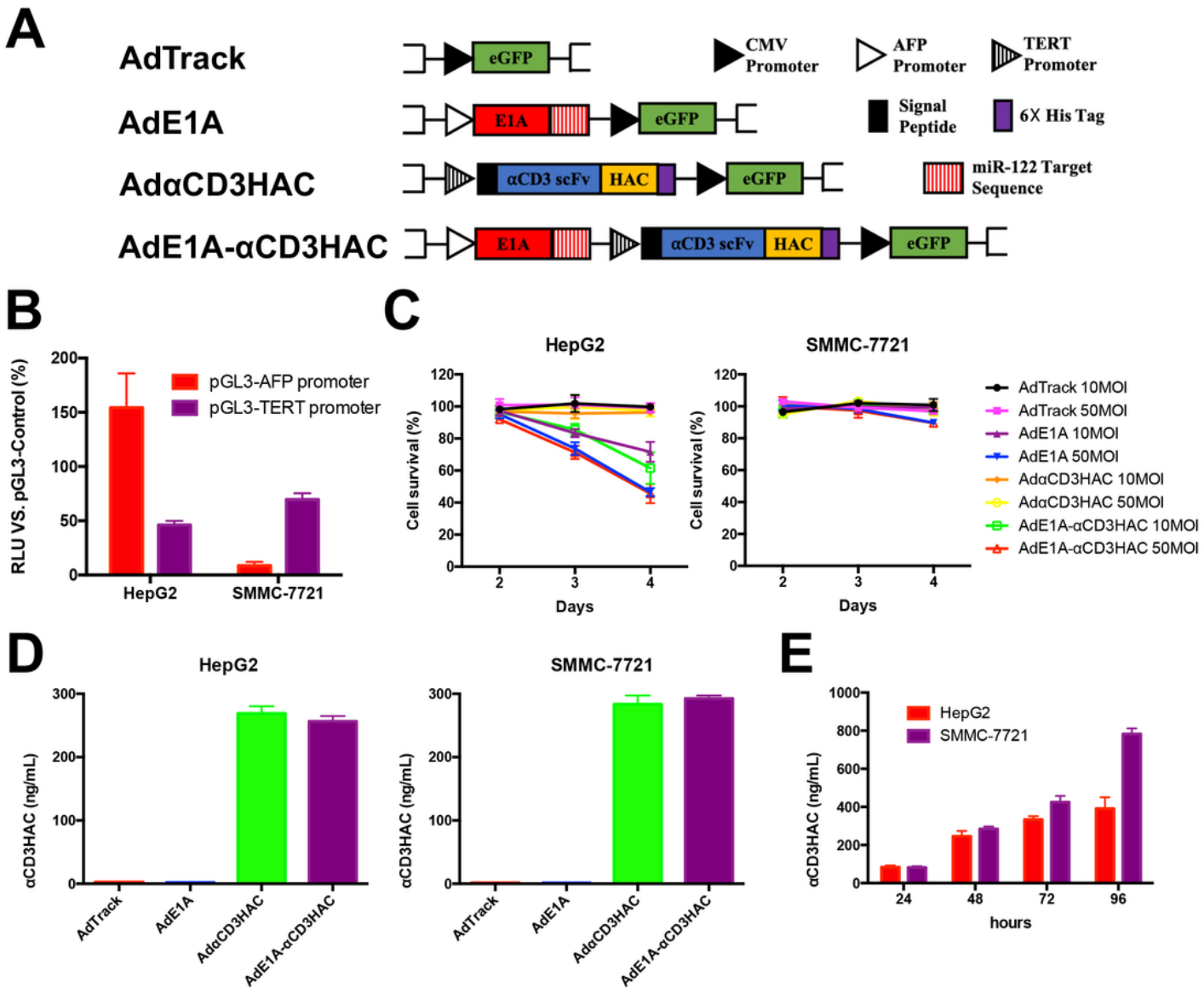

Fig. 1

Figure 1

Identification of the novel CRAd armed with αCD3HAC. A. The schematic representations of the novel CRAd (AdE1A-αCD3HAC) and its control adenoviruses. **B.** The transcriptional activities of AFP promoter and hTERT promoter in HepG2 and SMMC-7721 cell lines detected by Dual-luciferase® reporter system. **C.** The cell viabilities of HepG2 and SMMC-7721 after cells be infected with different adenoviruses at 10 or 50 MOI measured by CCK-8 assays **D.** The concentrations of αCD3HAC in culture supernatants of HepG2

and SMMC-7721 infected with different adenoviruses respectively at 50 MOI for 48 hours detected by ELISA assay. **E.** The concentrations of αCD3HAC in culture supernatants of HepG2 and SMMC-7721 infected with AdE1A-αCD3HAC at 50 MOI detected by ELISA assay every 24 hours. All these results represent the mean±SD for three separate experiments.

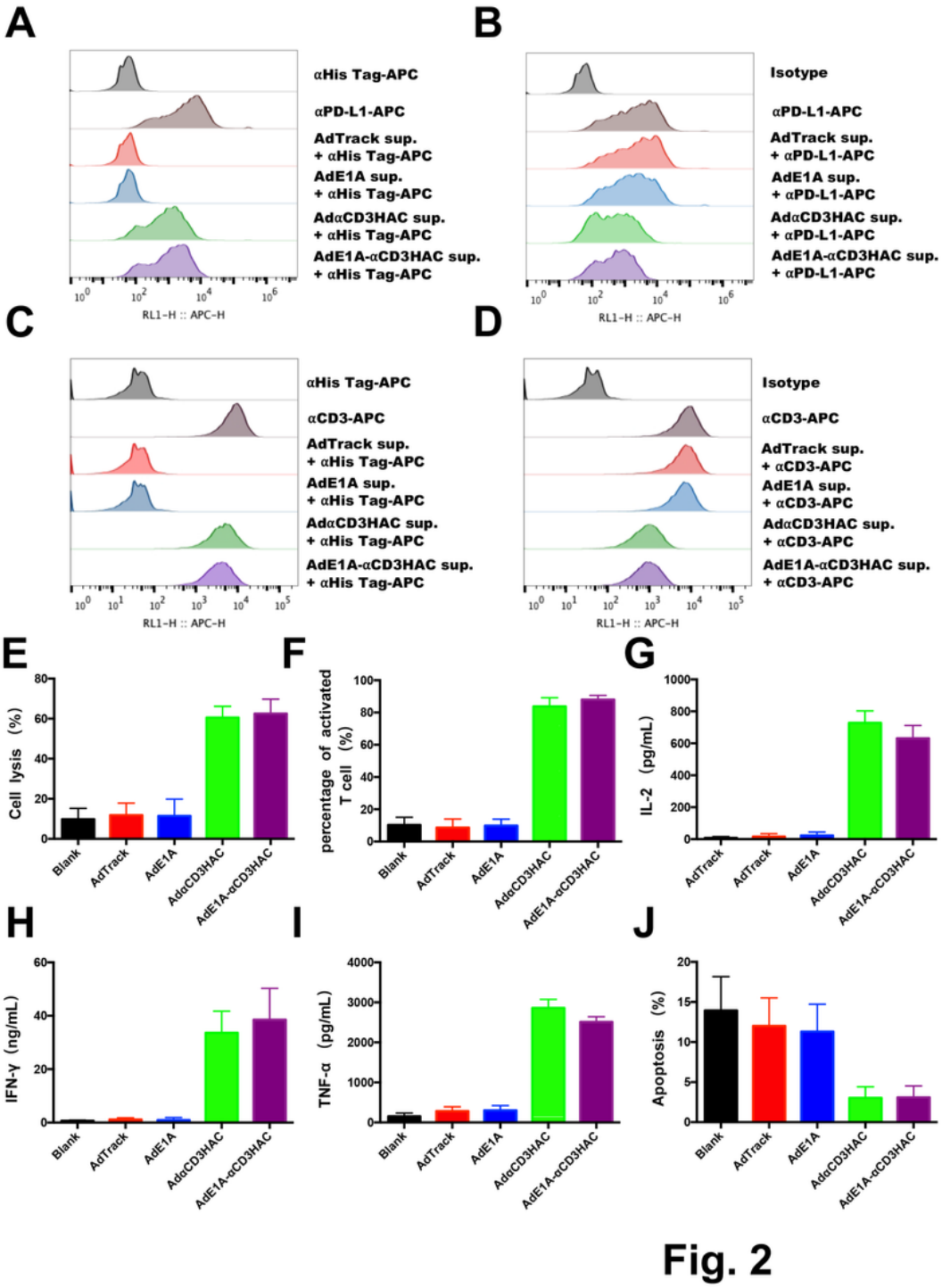

Fig. 2

Figure 2

Identification of αCD3HAC in culture supernatant. The culture supernatants of SMMC-7721 infected with different adenoviruses at 50 MOI respectively for 96 hours were collected for the direct binding assay and competitive binding assay (A-D). **A.** The direct binding activities of culture supernatants to PD-L1 detected by FACS on 7721-PD-L1 cell. APC-human PD-L1 antibody was used as positive control and APC-His tag antibody was used as second antibody. **B.** The competitive binding activities of culture supernatants with purchased APC-human PD-L1 antibody detected on 7721-PD-L1 cell by FACS. **C.** The direct binding activities of culture supernatants to human CD3 detected by FACS on Jurkat cell. APC-human CD3 antibody was used as positive control and APC-His tag antibody was used as second antibody. **D.** The competitive binding activities of culture supernatants with purchased APC-human CD3 antibody detected on Jurkat cell by FACS. **E.** PBMCs and 7721-PD-L1 cells were cocultured in the collected supernatants of infected SMMC-7721 at the ratio of 5:1 for 16 hours and the specific cytotoxicity toward 7721-PD-L1 cells was measured by lactate dehydrogenase assay using the CytoTox 96® nonradioactive cytotoxicity kit. **F.** The cell component in the coculture system was collected and stained with APC-human CD3 antibody and PE-human CD69 antibody for detecting activated T cells by FACS. **G-I.** The supernatants of the coculture system were measured by ELISA for the concentrations of IL-2, IFN-g and TNF-α. **J.** 7721-PD-L cell and Jurkat cell were cocultured in the collected supernatants of infected SMMC-7721 at the ratio of 10:1 for 24 hours. Then the cells were separated and stained with APC-human CD3 antibody and FITC-Annexin V. The apoptosis of Jurkat cell was measured by FASC. The results in E-J represent the mean±SD for three separate experiments.

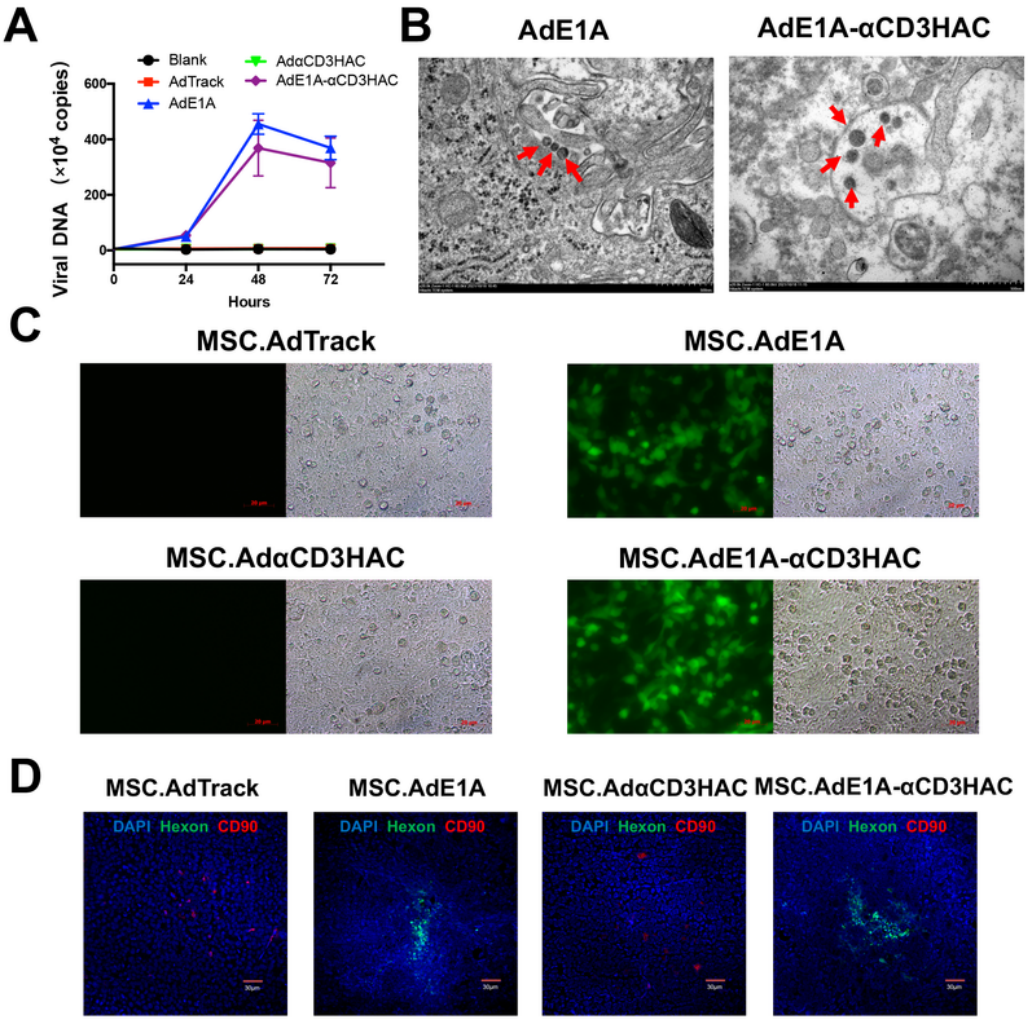

Fig. 3

Figure 3

Package and delivery of adenovirus by HUMSC. A. The DNA copy numbers of adenovirus in the hepatic differentiated HUMSC detected by real-time PCR at the indicated time after infection with different adenoviruses. This result represents the mean±SD for three separate experiments. **B.** The representative images of adenovirus particles in the hepatic differentiated HUMSC infected with AdE1A or AdE1A-αCD3HAC observed by electron microscope. Adenovirus particles were indicated by red arrows. Scar bar,

500 nm. **C.** The representative images of fluorescence microscope for HepG2 cells infected by the culture supernatants of the hepatic differentiated HUMSC infected with different adenoviruses. The supernatant containing adenovirus particles made HepG2 cells show green fluorescence. Scar bar, 20 μm. **D.** The representative images of confocal microscope for the tumor tissues of orthotopic hepatocarcinoma model mice treated by different MSC.Ads for 4 days. Green (anti-hexon protein) indicated adenvirus, red (anti-CD90) indicated HUMSC and blue (DAPI) indicated nuclei. Scar bar, 30 μm.

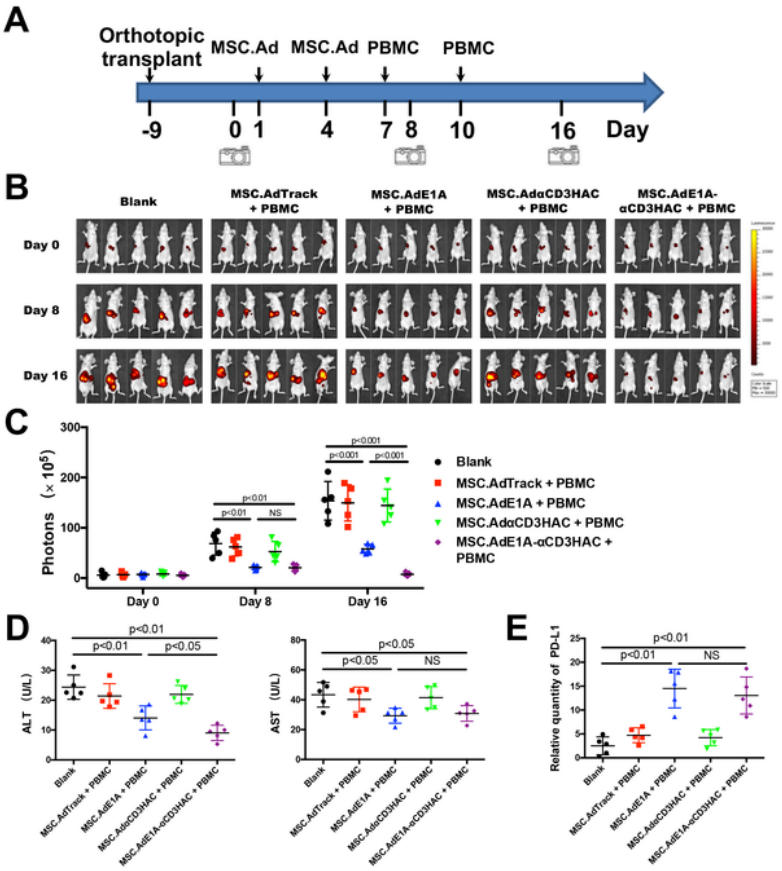

Fig. 4 Tumor suppression of MSC.AdE1A-αCD3HAC in combination with PBMC against liver orthotopic transplantation tumor. A. Design and timeline for therapeutic strategy. ( ) indicated the time for monitoring luciferase signal using Xenogen IVIS imaging system. **B.** IVIS images of HepG2-Luc cells were shown for all treatment groups (n=5 per group) at the indicated time. **C.** Quantification of luciferase signals on the all model mice at the indicated time. **D.** Levels of ALT and AST in the serum of the all model mice after treatment for 16 days. **E.** Relative quantity of PD-L1 expressed in the tumor tissues of all treatment groups detected by real-time PCR.

Figure 4

See image above for figure legend

Figure 5

Expression of αCD3HAC and activation of T cell in tumor tissue. A. The representative confocal microscope images for the tumor tissue of each treatment group on the 16th day. Green (anti-hexon protein) indicated adenovirus, red (anti-His tag) indicated αCD3HAC and blue (DAPI) indicated nuclei. Scar bar, 30 μm. **B.** The lymphocytes isolated from the tumor tissues of MSC.AdE1A+PBMC and MSC.AdE1A-αCD3HAC+PBMC treatment groups model mice (n=3 per group) were stained with APC-human CD3 antibody and PE-human CD69 antibody and analyzed by FACS. **C.** The statistical graph of the FACS assay on the percent of T cell in tumor. **D.** The statistical graph of the FACS assay on the percent of the activated T cell（$CD69^+$ $CD3^+$/ $CD3^+$）.

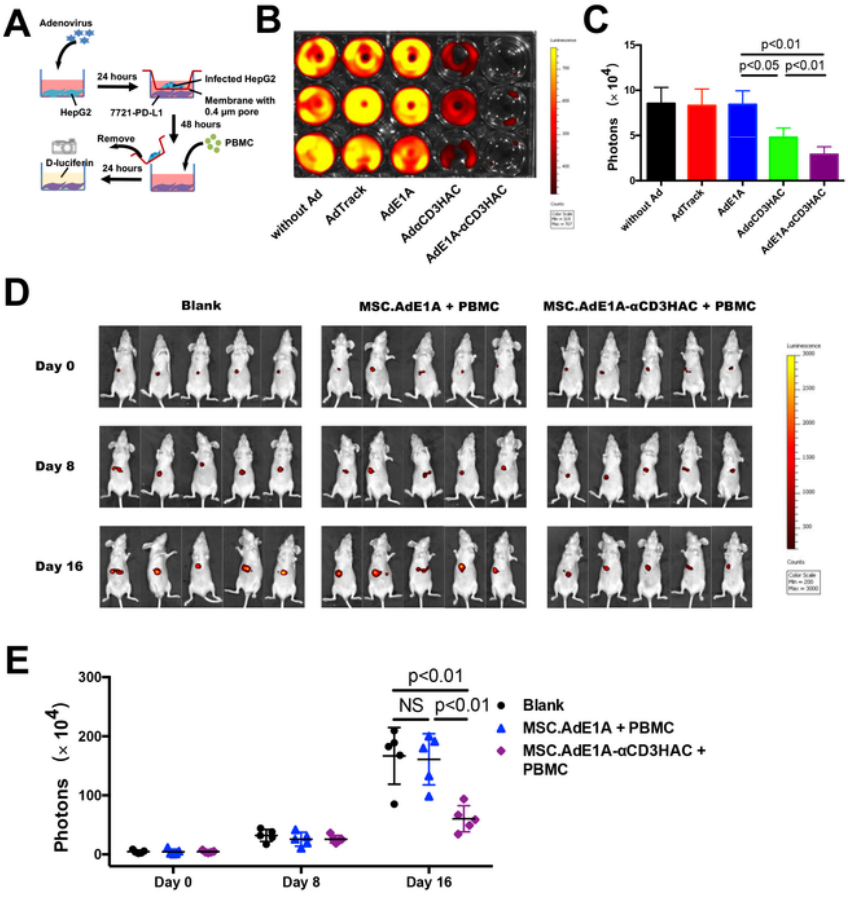

Fig. 6 Inhibitory effect on AFP heterogeneous hepatocarcinoma model. A. The schematic representation of the coculture and killing assay. ( ) indicated monitoring luciferase signal using Xenogen IVIS imaging system. **B.** The representative IVIS image of residual 7721-PD-L1 cells in the coculture and killing assay. **C.** Quantification of luciferase signals of the residual 7721-PD-L1 cells. **D.** The IVIS images of 7721-PD-L1 cells were shown for all treatment groups (n=5 per group) on AFP heterogeneous hepatocarcinoma model mice at the indicated time. **E.** Quantification of luciferase signals on the AFP heterogeneous hepatocarcinoma model mice at the indicated time.

Figure 6

See image above for figure legend

Supplementary Files

This is a list of supplementary files associated with this preprint. Click to download.

- Additionalfilelegend.docx
- FigS1.pdf
- FigS2.pdf
- FigS3.pdf
- FigS4.pdf
- FigS5.pdf
- FigS6.pdf
- FigS7.pdf
- FigS8.pdf
- FigS9.pdf